nature cell biology

Role of Bcl-2 family proteins in a non-apoptotic programmed cell death dependent on autophagy genes

Shigeomi Shimizu[1,2,3], Toku Kanaseki[4], Noboru Mizushima[4,5,6], Takeshi Mizuta[1,3], Satoko Arakawa-Kobayashi[4], Craig B. Thompson[7] and Yoshihide Tsujimoto[1,2,3,8]

Programmed cell death can be divided into several categories including type I (apoptosis) and type II (autophagic death)[1,2]. The Bcl-2 family of proteins are well-characterized regulators of apoptosis[3], and the multidomain pro-apoptotic members of this family, such as Bax and Bak, act as a mitochondrial gateway where a variety of apoptotic signals converge[4–6]. Although embryonic fibroblasts from Bax/Bak double knockout mice are resistant to apoptosis[4–6], we found that these cells still underwent a non-apoptotic death after death stimulation. Electron microscopic and biochemical studies revealed that double knockout cell death was associated with autophagosomes/autolysosomes. This non-apoptotic death of double knockout cells was suppressed by inhibitors of autophagy, including 3-methyl adenine, was dependent on autophagic proteins APG5 and Beclin 1 (capable of binding to Bcl-2/Bcl-x_L), and was also modulated by Bcl-x_L. These results indicate that the Bcl-2 family of proteins not only regulates apoptosis, but also controls non-apoptotic programmed cell death that depends on the autophagy genes.

It has been shown that cells lacking both Bax and Bak, the multidomain pro-apoptotic members of the Bcl-2 family, are completely resistant to apoptosis induced by various apoptotic stimuli, indicating that the multi-domain pro-apoptotic members act as a mitochondrial gateway for a variety of apoptotic signals[4–6]. However, although *Bax/Bak*$^{-/-}$ mice show several morphological abnormalities[4], programmed cell death seems to largely proceed in a normal manner, implying that a different mechanism compensates for apoptosis in these mice. Therefore, we investigated the response of cells from *Bax/Bak*$^{-/-}$ mice to various apoptotic stimuli in more detail.

When simian virus 40 (SV40)-transformed embryonic fibroblasts from *Bax/Bak*$^{-/-}$ mice (*Bax/Bak*$^{-/-}$ MEFs) were treated with etoposide (an inhibitor of topoisomerase II and a common apoptotic reagent), the cells became rounded, irregular and then ballooned (Fig. 1a; see Supplementary Information, Movie S1). We also continuously monitored these cells in the presence of propidium iodide (PI) (a membrane-impermeable stain for nucleic acids) under a fluorescent microscope. As shown in Fig. 1a, b and Supplementary Information, Movies S2 and S3, PI-positive cells were detected after 24 h and the majority of the cells were positively stained for PI by 48 h, indicating cell death. Note that the majority of PI-positive cells appeared to have been severely damaged. Consistently, when cell viability was assessed by the Resazurin reduction reaction using the Cell Titer Blue (CTB) assay, which measures the metabolic activity of viable cells in the same way as the MTT (methyl-thiazol-tetrazolium) assay, *Bax/Bak*$^{-/-}$ MEFs showed a significant decrease of viability (Fig. 1c). These results indicated that *Bax/Bak*$^{-/-}$ MEFs suffered a significant decrease of viability after etoposide treatment, although the extent of the change was smaller than in wild-type (WT) MEFs. As reported previously[4–6], etoposide-treated *Bax/Bak*$^{-/-}$ MEFs did not show any features of apoptosis (data not shown). Consistently, the addition of zVAD-fmk (a pan-caspase inhibitor) inhibited apoptosis of etoposide-treated WT MEFs, but did not improve the viability of *Bax/Bak*$^{-/-}$ MEFs (Fig. 1c).

To confirm the loss of cell viability after etoposide treatment, *Bax/Bak*$^{-/-}$ MEFs were exposed to etoposide, collected and re-cultured in standard medium. As shown in Fig. 1d, the proliferative activity of *Bax/Bak*$^{-/-}$ MEFs declined in a manner that was dependent on the duration of incubation with etoposide. Furthermore, the loss of cell viability was also confirmed by a clonogenicity (colony-forming) assay (Fig. 1e). Similar results were obtained when *Bax/Bak*$^{-/-}$ MEFs were treated with staurosporine (Fig. 1e and see Supplementary Information, Fig. S1a, b) or thapsigargin (data not shown). Moreover, etoposide and staurosporine induced a decrease of viability in primary *Bax/Bak*$^{-/-}$ MEFs and in thymocyte (see Supplementary Information, Fig. S1g, i, and data not shown). These results suggested that *Bax/Bak*$^{-/-}$ cells can be killed by various apoptosis-inducing reagents via a non-apoptotic process.

[1]Department of Post-Genomics & Diseases, Osaka University Medical School, [2]CREST and [3]SORST of the Japan Science and Technology Corporation (JST), 2-2 Yamadaoka, Suita, Osaka 565-0871, Japan. [4]Department of Cell Biology, National Institute for Basic Biology, and [5]PRESTO of the Japan Science and Technology Corporation (JST), Okazaki, Aichi 444-8585, Japan. [6]Department of Bioregulation and Metabolism, The Tokyo Metropolitan Institute of Medical Science, Tokyo 113-8613, Japan. [7]Departments of Medicine and Cancer Biology, Abramson Family Cancer Research Institute, University of Pennsylvania, Philadelphia, PA 19104 USA. [8]Correspondence should be addressed to: Y.T. (e-mail: tsujimot@gene.med.osaka-u.ac.jp)

Published online: 21 Novmeber 2004, DOI: 10.1038/ncb1192

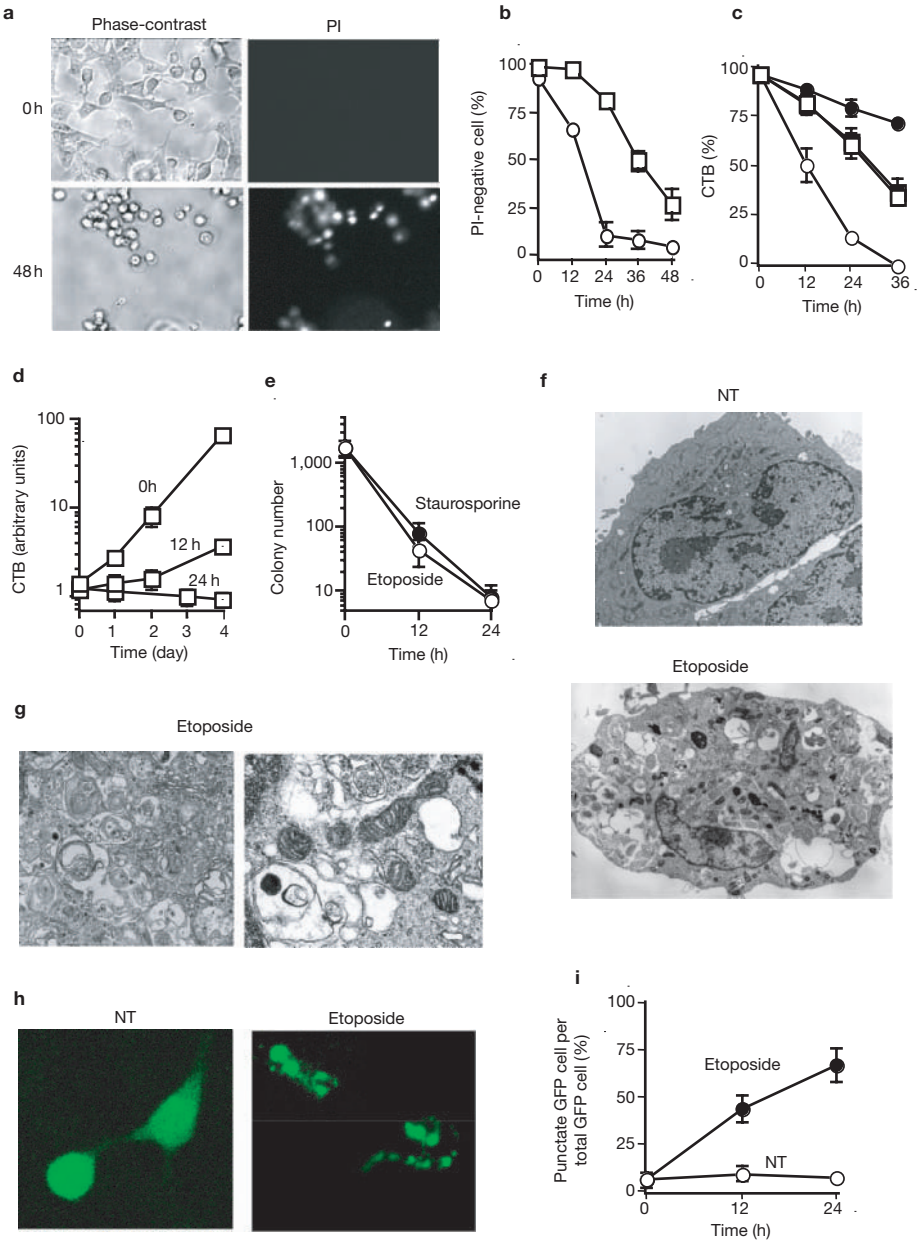

Figure 1 Loss of viability of and induction of autophagy in Bax/Bak$^{-/-}$ MEFs exposed to etoposide and staurosporine. (**a**) Representative photographs of Bax/Bak$^{-/-}$ MEFs treated with etoposide. Bax/Bak$^{-/-}$ MEFs were treated with 20 μM etoposide in the presence of PI (2 μM) for the indicated times, and were analysed under a phase-contrast and fluorescence (PI) microscope. (**b**, **c**) Reduced viability of Bax/Bak$^{-/-}$ MEFs after exposure to etoposide. WT (circles) and Bax/Bak$^{-/-}$ (squares) MEFs were treated with 20 μM etoposide in the presence (closed symbols) or absence (open symbols) of 100 μM zVAD-fmk. Then cell viability was measured by the PI staining (**b**) and CTB assay (**c**), and expressed as a percentage of the initial value without etoposide. Data are shown as mean ± s.d. ($n = 4$). (**d**) Reduced viability of etoposide-treated Bax/Bak$^{-/-}$ MEFs as assessed by proliferation assay. Bax/Bak$^{-/-}$ MEFs were either not treated (0 h) or were treated with 20 μM etoposide for 12 and 24 h, then all cells were recovered and 5,000 cells were reseeded. Viable cell numbers were measured on the indicated days by the CTB assay. Results were normalized by adjusting the day 0 value. $n = 4$. (**e**) Reduced viability of Bax/Bak$^{-/-}$ MEFs after exposure to etoposide and staurosporine, as assessed by clonogenicity assay. MEFs were treated with etoposide (20 μM) or staurosporine (1 μM) at the indicated times, collected, and 2,000 cells were seeded in the normal medium. After 1 week, colonies were counted. $n = 4$. (**f**–**i**) Induction of autophagy in Bax/Bak$^{-/-}$ MEFs by etoposide. (**f**) Electron micrograph (×14,800) of Bax/Bak$^{-/-}$ MEF treated with etoposide (20 μM) for 18 h. Representative features of Bax/Bak$^{-/-}$ MEFs that have received no treatment (NT; that is, are healthy) are also shown (NT: ×14,000). (**g**) In magnified photographs, a large number of autolysosomes/autophagosomes (left: ×26,000) were observed, but the mitochondria were unaffected (right: ×17,000). (**h**, **i**) Punctate GFP–LC3 fluorescence in Bax/Bak$^{-/-}$ MEFs treated with etoposide. GFP–LC3-transfected cells were incubated with and without etoposide (20 μM) for 24 h (**h**) or the indicated times (**i**), and then examined by fluorescent microscopy. (**h**) Representative photographs of healthy (NT) and etoposide-treated Bax/Bak$^{-/-}$ MEFs are shown. (**i**) The percentage of cells with punctate GFP–LC3 fluorescence was calculated relative to all GFP-positive cells. Data are shown as mean ± s.d. ($n = 4$).

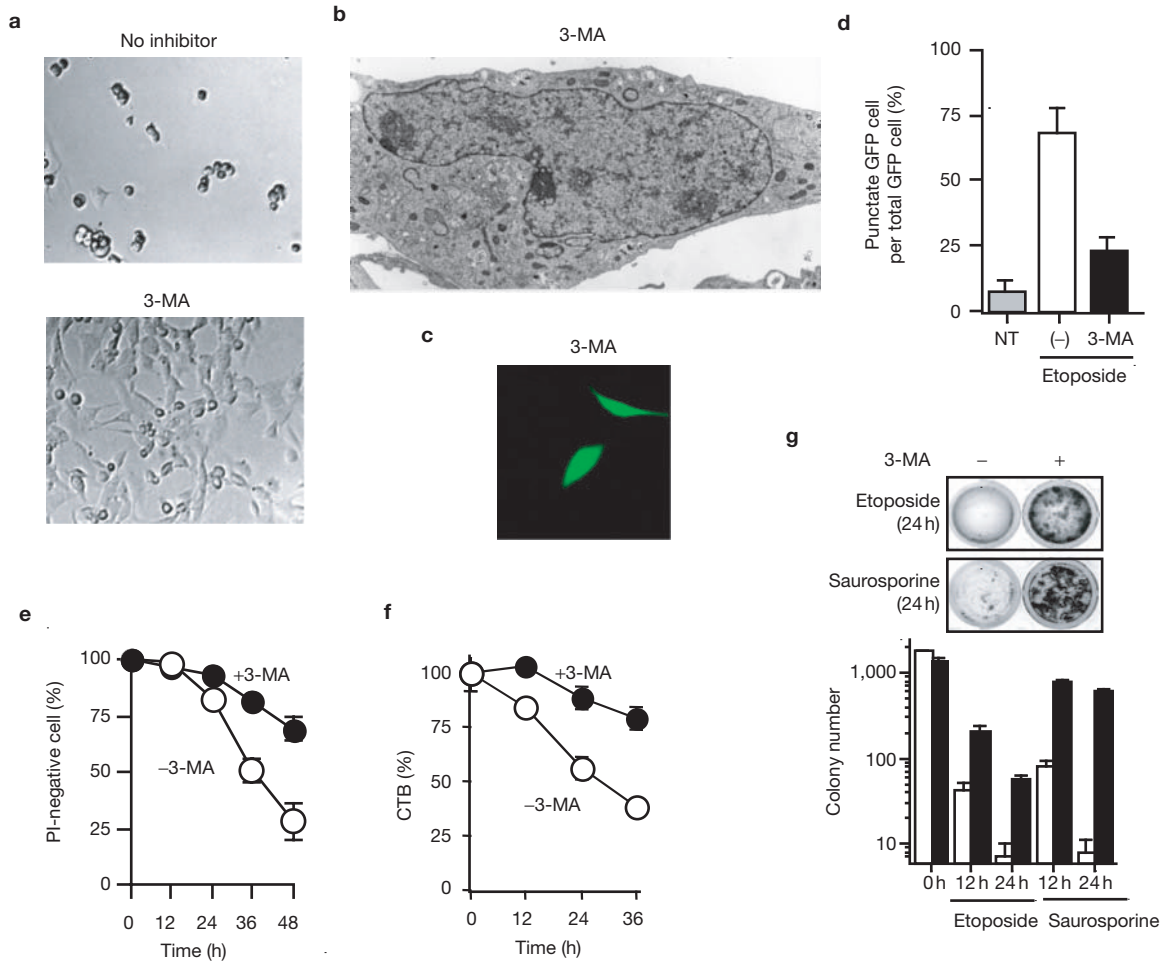

Figure 2 Inhibition of etoposide-induced death of Bax/Bak$^{-/-}$ MEFs by 3-MA. (**a**, **b**) Bax/Bak$^{-/-}$ MEFs were treated with 20 μM etoposide in the absence or presence of 10 mM 3-MA for 24 h, and then were examined by phase-contrast microscopy (**a**) and electron microscopy (×8,400) (**b**). Autolysosomes/autophagosomes were hardly observed. (**c**, **d**) Reduction of punctate GFP–LC3 fluorescence in Bax/Bak$^{-/-}$ MEFs by 3-MA. Bax/Bak$^{-/-}$ MEFs that were transfected with GFP–LC3 were incubated without (NT) or with 20 μM etoposide in the presence or absence of 10 mM 3-MA for 24 h, and then were examined by confocal fluorescent microscopy. (**c**) Representative photograph of etoposide-treated Bax/Bak$^{-/-}$ MEFs in the presence of 3-MA. (**d**) The percentage of cells with punctate GFP–LC3 fluorescence was calculated relative to all GFP–LC3-positive cells. Data are shown as mean ± s. d. ($n = 4$). (**e**–**g**) Inhibition of etoposide- and staurosporine-induced cell death by 3-MA. Bax/Bak$^{-/-}$ MEFs were treated with 20 μM etoposide (**e**–**g**) or 1 μM staurosporine (**g**) in the absence (open symbols) or presence (closed symbols) of 10 mM 3-MA for the indicated time. Cell viability was measured by PI staining (**e**), CTB assay (**f**) and clonogenicity assay (**g**) (as in Fig. 1e). Upper panels in **g**: viable cells were visualized by staining with calcein-AM. $n = 4$.

To investigate the mechanism underlying the death of *Bax/Bak*$^{-/-}$ MEFs induced by apoptotic stimuli, the cells were examined by electron microscopy. As shown in Fig. 1f, g, the majority of etoposide-treated *Bax/Bak*$^{-/-}$ MEFs, but not healthy MEFs, contained a number of autophagosomes/autolysosomes, which are a characteristic feature of autophagy. Moreover, a significant number of cells appeared to have undergone destruction by abundant autophagosomes/autolysosomes, raising the possibility that an autophagic process might be involved in the non-apoptotic death of *Bax/Bak*$^{-/-}$ MEFs. In contrast, many of the mitochondria appeared normal (Fig. 1g), although some were found inside the autophagosomes (data not shown). Although the nuclei were deformed, neither chromatin condensation nor nuclear fragmentation was observed (Fig. 1f), confirming the absence of apoptotic cell death. Autophagy is a pathway for the bulk degradation of subcellular constituents through the creation of autophagosomes/autolysosomes in response to stresses such as nutrient deprivation[7]. In general, autophagy is utilized so that cells can survive, but constitutive activation of autophagy may induce cell death. To visualize autophagy, green fluorescent protein (GFP)-tagged light-chain 3 (LC3) (ref. 8) was expressed in *Bax/Bak*$^{-/-}$ MEFs. During the autophagic process, LC3 is concentrated in autophagosomes, so the punctate fluorescence produced by GFP–LC3 can be used as a good indicator of autophagy[8]. As shown in Fig. 1h, diffuse cytoplasmic localization of GFP–LC3 was observed in healthy *Bax/Bak*$^{-/-}$ MEFs, whereas etoposide-treated *Bax/Bak*$^{-/-}$ MEFs showed punctuate fluorescence. The number of cells with punctate GFP–LC3 fluorescence increased in a time-dependent manner after etoposide treatment (Fig. 1i). Similar findings were also observed when *Bax/Bak*$^{-/-}$ MEFs were treated with staurosporine (see Supplementary Information, Fig. S1c, d). All of these results indicated that apoptotic stimuli could induce non-apoptotic death of *Bax/Bak*$^{-/-}$ MEFs, which was associated with the generation of autophagosomes/autolysosomes.

To elucidate the involvement of the autophagic process in non-apoptotic death of *Bax/Bak*$^{-/-}$ MEFs, the effects of several inhibitors of autophagy were tested. Autophagy is known to be inhibited by PI3 kinase inhibitors,

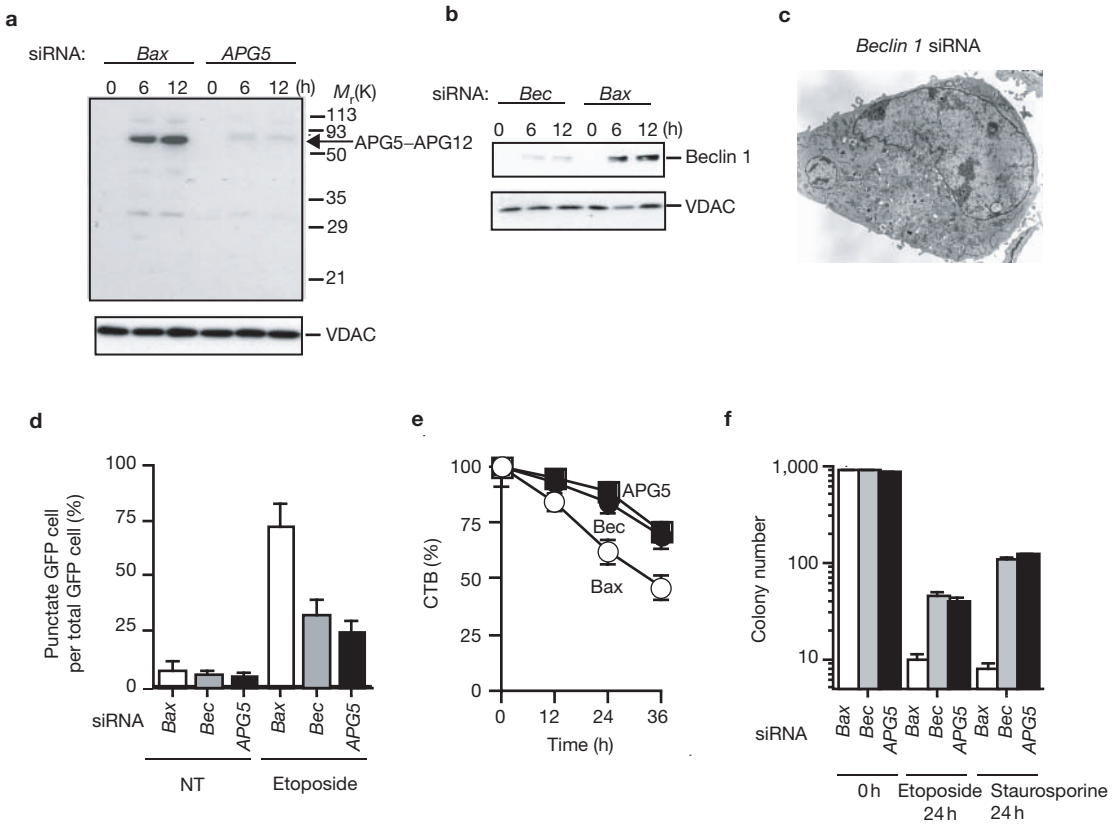

Figure 3 Inhibition of etoposide-induced death of Bax/Bak$^{-/-}$ MEFs by silencing autophagy genes. (**a**, **b**) Bax/Bak$^{-/-}$ MEFs were treated with the indicated siRNAs (10 μg) for 24 h and then incubated with 20 μM etoposide for the indicated times. Expression of APG5–APG12 complex (**a**), Beclin 1 (**b**) and VDAC (loading control) was analysed by Western blot analysis. (**c**) Inhibition of etoposide-induced autophagy by silencing of Beclin 1. Bax/Bak$^{-/-}$ MEFs with silencing of Beclin 1 were treated with 20 μM etoposide at 18 h and were analysed by electron microscopy (×8,500). (**d**) Reduction of punctate GFP–LC3 fluorescence in Bax/Bak$^{-/-}$ MEFs by silencing of Beclin 1 and APG5. Bax/Bak$^{-/-}$ MEFs that were transfected with GFP–LC3 together with the indicated siRNAs, were incubated without (NT) or with 20 μM etoposide for 24 h, and then examined by confocal fluorescent microscopy. The percentage of cells with punctate GFP–LC3 fluorescence was calculated relative to all GFP–LC3-positive cells. Data are shown as mean ± s.d. ($n = 4$). (**e**, **f**) Inhibition of etoposide- and staurosporine-induced cell death by silencing of Beclin 1 and APG5. Bax/Bak$^{-/-}$ MEFs that were treated with the indicated siRNAs were incubated with 20 μM etoposide (**e**, **f**) or 1 μM staurosporine (**f**) for the indicated time. Cell viability was measured by CTB assay (**e**) and clonogenicity assay (**f**). $n = 4$.

such as 3-methyladenine (3-MA) and wortmannin[7]. When *Bax/Bak*$^{-/-}$ MEFs were treated with etoposide in the presence of 3-MA, cell rounding and detachment were almost completely inhibited (Fig. 2a). Etoposide-induced development of autophagosomes/autolysosomes was also inhibited by 3-MA (Fig. 2b–d). Cell viability was markedly improved by 3-MA, as shown by PI staining (Fig. 2e; see Supplementary Information, Movies S4 and S5), the CTB assay (Fig. 2f) and a clonogenicity assay (Fig. 2g). Similar results were obtained with wortmannin (data not shown). Note that incubation with 3-MA or wortmannin showed only slight toxicity to cells (5–10% reduction of cell viability in 24 h). Because we used low concentrations of these drugs for all subsequent studies, toxicity should not be an issue. 3-MA also inhibited staurosporine-induced death of *Bax/Bak*$^{-/-}$ MEFs (Fig. 2g and see Supplementary Information, Fig. S1e, f), and non-apoptotic death induced by etoposide and staurosporine in primary *Bax/Bak*$^{-/-}$ MEFs and thymocytes (see Supplementary Information, Fig. S1h, i, and data not shown).

For further confirmation of the involvement of an autophagic process in the non-apoptotic death of *Bax/Bak*$^{-/-}$ MEFs, we used gene silencing with short interfering RNA (siRNA) to inhibit some genes related to the autophagic process. The protein APG5 is essential for the generation of autophagosomes by covalent binding to APG12 (ref. 9). Beclin 1 is part of a class III PI3 kinase complex that is also crucial for autophagy[10], and may function upstream of other APG proteins[11]. Interestingly, when *Bax/Bak*$^{-/-}$ MEFs were treated with etoposide, there was considerable accumulation of both the APG5–APG12 complex and Beclin 1 (Fig. 3a, b), consistent with induction of the autophagic process in etoposide-treated *Bax/Bak*$^{-/-}$ MEFs. Accumulation of Beclin 1 and the APG5–APG12 complex was inhibited by silencing of the respective genes (Fig. 3a, b). We used *Bax* siRNA as a control because Bax was absent in *Bax/Bak*$^{-/-}$ MEFs. Etoposide-induced generation of autophagosomes/autolysosomes was markedly inhibited by silencing of Beclin 1 and APG5 (Fig. 3c, d, and data not shown). Silencing of Beclin 1 and APG5 reduced the etoposide-induced death of *Bax/Bak*$^{-/-}$ MEFs (Fig. 3e, f). Similar results were obtained when cells were treated with staurosporine (Fig. 3f). All of these findings indicated that various apoptotic stimuli could induce non-apoptotic death of *Bax/Bak*$^{-/-}$ MEFs, which was dependent on autophagy genes.

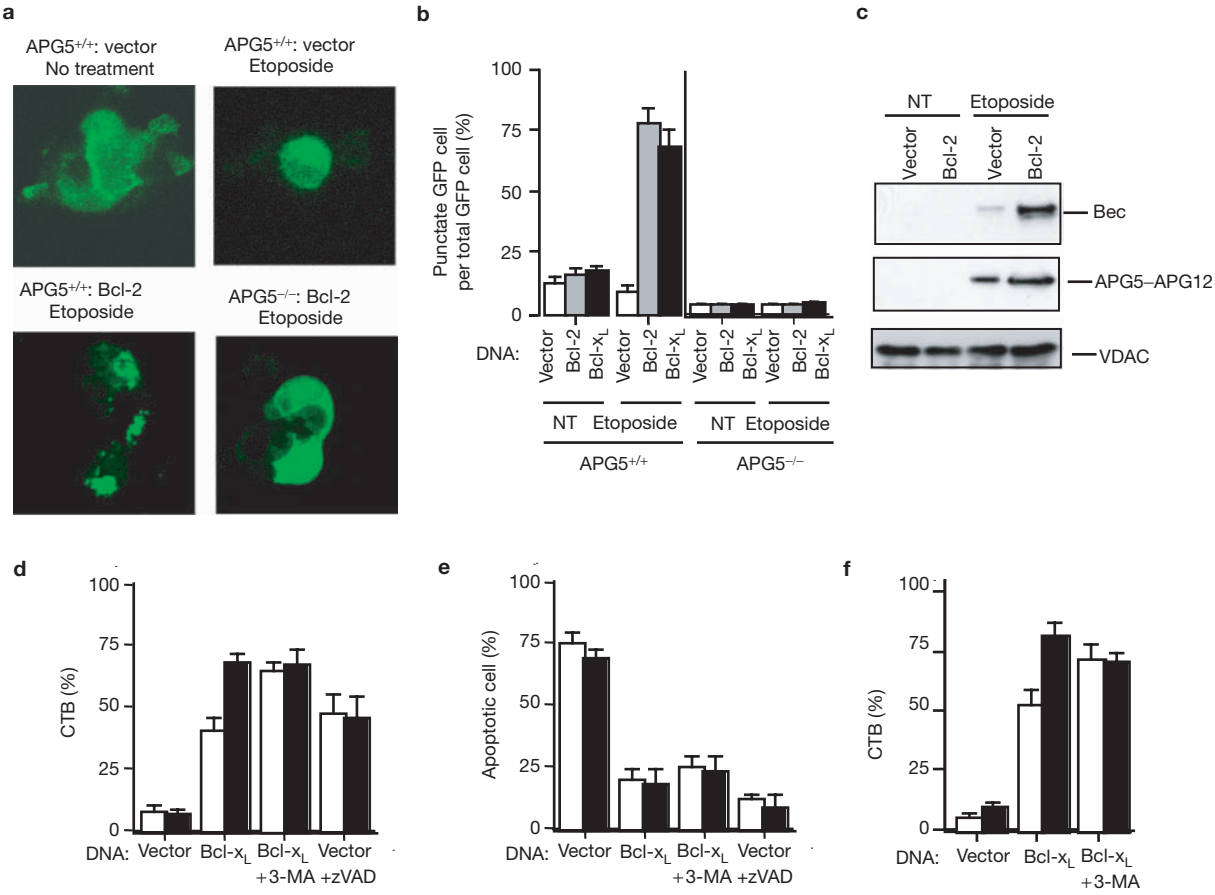

Figure 4 Occurrence of etoposide-induced, 3-MA-inhibitable, non-apoptotic death in MEFs by overexpressed Bcl-2/Bcl-x_L. (**a**, **b**) APG5-dependent punctate GFP–LC3 fluorescence in Bcl-2-transfected MEFs after etoposide treatment. $APG5^{+/+}$ and $APG5^{-/-}$ MEFs that were transfected with both GFP–LC3 and the indicated plasmids (Bcl-2 or vector) were incubated without or with 20 μM etoposide for 24 h, then examined by confocal fluorescent microscopy (**a**). The percentage of cells with punctate GFP–LC3 fluorescence was calculated relative to all GFP–LC3-positive cells (**b**). (**c**) Accumulation of Beclin 1 and APG5–APG12 complex in Bcl-2-transfected MEFs after etoposide treatment. WT MEFs were transfected with the indicated plasmids, and were incubated without (NT) or with 20 μM etoposide for 24 h. (**d**, **e**) Occurrence of etoposide-induced 3-MA-inhibitable non-apoptotic death in Bcl-x_L-overexpressing $APG5^{+/+}$ MEFs, but not $APG5^{-/-}$ MEFs. $APG5^{+/+}$ (open columns) and $APG5^{-/-}$ (closed columns) MEFs were transfected with the indicated plasmids (2 μg). After 24 h, transfected cells were incubated with 20 μM of etoposide in the presence or absence of 100 μM of zVAD or 10 mM of 3-MA for 24 h, and cell viability was measured by the CTB assay (**d**) and apoptotic nuclear morphology (**e**). Data are shown as mean ± s.d. ($n = 4$). (**f**) Overexpression of Bcl-x_L does not sensitize Beclin 1-silenced MEFs to etoposide-induced 3-MA-inhibitable non-apoptotic death. WT MEFs with silencing of control GFP (open columns) or Beclin 1 (closed columns) were transfected with the indicated plasmids (1 μg). After 24 h, transfected cells were incubated with 20 μM of etoposide in the presence or absence of 10 mM of 3-MA for 24 h, and cell viability was measured by the CTB assay. $n = 3$.

To confirm that apoptotic stimulation induced non-apoptotic cell death in *Bax/Bak*$^{-/-}$ MEFs owing to the absence of Bax and Bak, either Bax or Bak was expressed in these cells and then treatment with etoposide was performed. In contrast to *Bax/Bak*$^{-/-}$ MEFs, Bax- (or Bak)-transfected *Bax/Bak*$^{-/-}$ MEFs developed certain features of apoptosis, and were inhibited by zVAD-fmk, but not by 3-MA (see Supplementary Information, Fig. S2a, b). Thus, etoposide-induced non-apoptotic death of *Bax/Bak*$^{-/-}$ MEFs was a consequence of the inhibition of Bax/Bak activity.

To show that non-apoptotic death was not a simple consequence of the inhibition of apoptosis, we next examined non-apoptotic death in zVAD-added WT MEFs, and Apaf-1- and caspase-9-deficient MEFs after treatment with etoposide. In all cases, a small (but significant) decrease of cell viability was detected, but this decrease was not inhibited by 3-MA (see Supplementary Information, Fig. S2c–f). Furthermore, etoposide-treated WT MEFs showed only mild autophagic manifestations (see Supplementary Information, Fig. S2g–i), indicating that the 3-MA-inhibitable non-apoptotic death of *Bax/Bak*$^{-/-}$ MEFs was not merely due to inhibition of apoptosis, but was related to deficiency of both Bax and Bak.

We next examined the effect of overexpression of Bcl-2 and Bcl-x_L in WT MEFs. These cells were expected to undergo 3-MA-inhibitable non-apoptotic death, as do *Bax/Bak*$^{-/-}$ MEFs in response to apoptotic stimulations. MEFs overexpressing Bcl-2 (and also Bcl-x_L) showed punctuate GFP–LC3 fluorescence (Fig. 4a, b) and greater accumulation of Beclin 1 and APG5–APG12 complex after etoposide treatment than did WT MEFs (Fig. 4c). This punctuate GFP–LC3 fluorescence was not observed in *APG5*$^{-/-}$ MEFs (Fig. 4a, b), in which autophagy was impaired[18], indicating that overexpression of Bcl-2/Bcl-x_L induced APG5-dependent autophagy in WT MEFs after etoposide treatment. To confirm that cells overexpressing Bcl-2/Bcl-x_L undergo etoposide-induced non-apoptotic death, *APG5*$^{-/-}$ MEFs were transfected with a

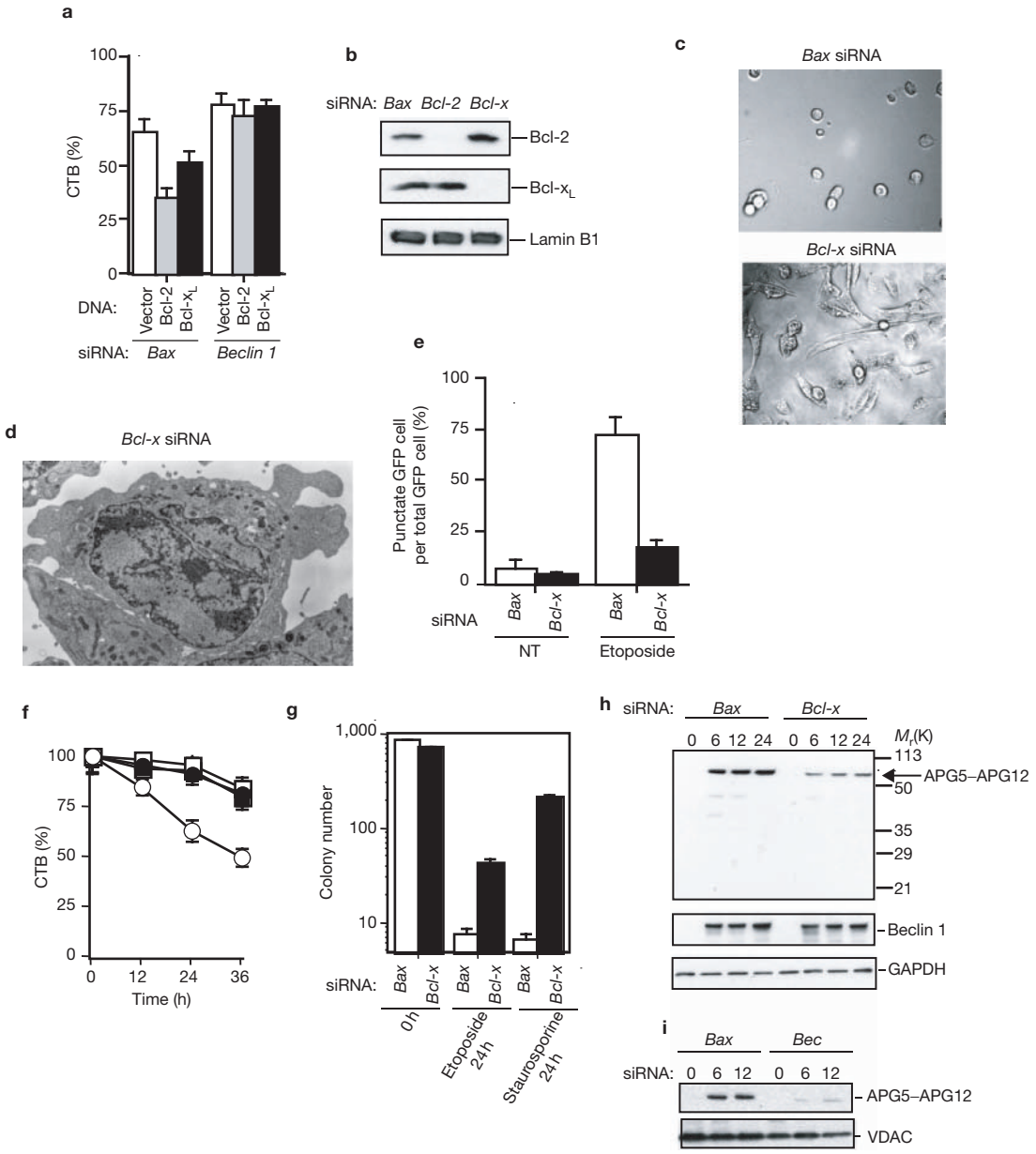

Figure 5 Inhibition of non-apoptotic death in etoposide-treated Bax/Bak$^{-/-}$ MEFs by siRNA for Bcl-x. (**a**) Enhancement of etoposide-induced non-apoptotic death by overexpression of human Bcl-2 and Bcl-x_L in Bax/Bak$^{-/-}$ MEFs in a Beclin 1-dependent manner. Bax/Bak$^{-/-}$ MEFs with silencing of control Bax or Beclin 1 were transfected with the indicated plasmids (1 μg). After 24 h, the transfected cells were incubated with 20 μM etoposide for 24 h, and cell viability was assessed by the CTB assay. Data are shown as mean ± s.d. ($n = 3$). (**b**) Bax/Bak$^{-/-}$ MEFs were transiently transfected with 10 μg of siRNA for Bcl-2, Bcl-x, or Bax (negative control) for 24 h. Expression levels of Bcl-2, Bcl-x_L and Lamin B (loading control) were analysed by Western blot analysis. (**c**–**e**) Inhibition of etoposide-induced autophagy in Bax/Bak$^{-/-}$ cells treated with siRNA for Bcl-x. (**c**) Bax/Bak$^{-/-}$ MEFs that were transfected with the indicated siRNAs were treated with 20 μM etoposide for 24 h, then examined by phase-contrast microscopy. (**d**) Bax/Bak$^{-/-}$ MEFs that were transfected with siRNA for Bcl-x and then treated with etoposide for 18 h were analysed by electron microscopy (×8,500). (**e**) Reduction of punctate GFP–LC3 fluorescence in etoposide-treated Bax/Bak$^{-/-}$ MEFs by silencing of Bcl-x. Bax/Bak$^{-/-}$ MEFs that were transfected with both GFP–LC3 and the indicated siRNAs were incubated without (NT) or with etoposide for 24 h, and then were examined by confocal fluorescent microscopy. The percentage of cells with punctate GFP–LC3 fluorescence was calculated relative to all GFP–LC3-positive cells. $n = 4$. (**f**) Inhibition of etoposide-induced cell death by silencing of Bcl-x. Bax/Bak$^{-/-}$ MEFs were transfected with siRNA (circles, siRNA for Bax; squares, siRNA for Bcl-x) were treated with 20 μM etoposide in the absence (open symbols) or presence (closed symbols) of 10 mM 3-MA, and cell viability was assessed by the CTB assay at the indicated times. $n = 4$. (**g**) Clonogenicity assay of Bax/Bak$^{-/-}$ MEFs after exposure to etoposide and staurosporine. Bax/Bak$^{-/-}$ MEFs that were transfected with the indicated siRNAs were treated with 20 μM etoposide or 1 μM staurosporine at 24 h. After collection, 2,000 cells were seeded in the normal medium. After one week, colonies were counted. (**h**, **i**) Inhibition of APG5–APG12 induction by silencing of Bcl-x or Beclin 1. Bax/Bak$^{-/-}$ MEFs were treated with the indicated siRNAs (10 μg) for 24 h and then incubated with 20 μM etoposide for the indicated times. Expression of APG5–APG12 complex, Beclin 1 and GAPDH/VDAC (loading control) was analysed by Western blot analysis.

Bcl-x_L-expressing plasmid and then treated with etoposide. As shown in Fig. 4d, the viability of Bcl-x_L-expressing *APG5*$^{-/-}$ MEFs was superior to that of Bcl-x_L-expressing *APG5*$^{+/+}$ MEFs, and the latter was increased by 3-MA. In both types of cells, apoptosis was similarly inhibited (Fig. 4e). Thus, whereas overexpression of Bcl-x_L clearly increased the survival of both *APG5*$^{+/+}$ and *APG5*$^{-/-}$ cells, Bcl-x_L overexpression increased the difference in cell death between *APG5*$^{+/+}$ and *APG5*$^{-/-}$ cells, which would be predicted to be the autophagic component. In contrast to Bcl-x_L, vector DNA transfection did not produce any difference between the viability of *APG5*$^{-/-}$ MEFs and *APG5*$^{+/+}$ MEFs, irrespective of the presence of zVAD-fmk (Fig. 4d). Similar findings were obtained when Bcl-2-expressing plasmid was used (data not shown). Non-apoptotic death observed in MEFs with overexpressed Bcl-2/Bcl-x_L was not seen when Beclin 1 was silenced (Fig. 4f). These data suggested that overexpression of Bcl-2 or Bcl-x_L not only inhibited apoptosis, but also sensitized at least a fraction of cells to non-apoptotic death dependent on autophagy genes (such as Bax/Bak-deficiency); however, we could not formally exclude the possibility that overexpression of Bcl-2 and Bcl-x_L simply increases the efficiency of autophagosome formation, which may not necessarily be translated into more cell death, and that APG5 and Beclin 1 are relevant modulators of cell death.

In the *Bax/Bak*$^{-/-}$ cells, apoptotic reagents induced non-apoptotic cell death, which was dependent on genes related to autophagy, including Beclin 1. Beclin 1 interacts with Bcl-2/Bcl-x_L (but not Bax/Bak)[12], raising the possibility that Bcl-2/Bcl-x_L may have a role in the non-apoptotic death of *Bax/Bak*$^{-/-}$ MEFs. We first examined the effect of overexpression of Bcl-2 and Bcl-x_L in *Bax/Bak*$^{-/-}$ MEFs. As expected, overexpression of Bcl-2 and Bcl-x_L in *Bax/Bak*$^{-/-}$ MEFs resulted in enhancement of the non-apoptotic death, which was cancelled by silencing of Beclin 1 (Fig. 5a). We next examined the effect of silencing these molecules in *Bax/Bak*$^{-/-}$ MEFs by using siRNA. Endogenous Bcl-2 and Bcl-x_L were almost completely eliminated from *Bax/Bak*$^{-/-}$ MEFs by the respective siRNAs (Fig. 5b). Despite etoposide treatment, a large fraction of the Bcl-x-silenced *Bax/Bak*$^{-/-}$ MEFs appeared healthy (Fig. 5c) and the creation of autophagosomes was markedly suppressed (Fig. 5d, e). The majority of the cells remained viable irrespective of the addition of 3-MA (Fig. 5f), indicating that the non-apoptotic death was not induced and suggesting that Bcl-x_L was required for the non-apoptotic death of *Bax/Bak*$^{-/-}$ MEFs. As expected in the absence of Bax/Bak, these cells did not undergo apoptotic death (data not shown). In contrast to the silencing of Bcl-x, silencing of Bcl-2 did not have any effect (see Supplementary Information, Fig. S2j, k)—probably not owing to functional differences between Bcl-2 and Bcl-x, but to the much lower level of Bcl-2 than Bcl-x_L expression in MEFs—because Bcl-2 overexpression cancelled the effect of Bcl-x silencing (see Supplementary Information, Fig. S2l). The improved viability after Bcl-x silencing was also confirmed by a clonogenicity assay (Fig. 5g). As shown in Fig. 5h, the etoposide-induced increase of Beclin 1 in Bcl-x-silenced *Bax/Bak*$^{-/-}$ MEFs was similar to that in control *Bax/Bak*$^{-/-}$ MEFs, whereas induction of APG5–APG12 was far weaker in Bcl-x-silenced *Bax/Bak*$^{-/-}$ MEFs than in control *Bax/Bak*$^{-/-}$ MEFs. Because Beclin 1 binds to Bcl-x_L, and silencing of Beclin 1 reduced the APG5–APG12 level (Fig. 5i), Bcl-x_L might be required for induction of APG5–APG12 through regulation of Beclin 1.

Because *Bax/Bak*$^{-/-}$ MEFs lost viability after exposure to apoptotic stimuli in an autophagic protein-dependent and 3-MA-inhibitable manner, it might be assumed that this type of non-apoptotic death is similar to death induced by nutrient starvation, which also activates the autophagic process. However, etoposide/staurosporine-induced non-apoptotic death of *Bax/Bak*$^{-/-}$ cells showed substantial differences from death induced by amino-acid starvation on the basis of the following findings: (1) whereas etoposide/staurosporine-induced non-apoptotic death of *Bax/Bak*$^{-/-}$ is inhibited by 3-MA, amino-acid starvation-induced death is not inhibited, but rather is enhanced by 3-MA (see Supplementary Information, Fig. S3a, b), probably owing to an impaired supply of amino acids; (2) amino-acid starvation induces apoptosis in WT cells that are dependent on Bax/Bak (see Supplementary Information, Fig. S3b); and (3) accumulation of Beclin 1 and APG5–APG12 was observed in cells undergoing etoposide/staurosporine-induced non-apoptotic death, but not in cells that died of amino-acid starvation (see Supplementary Information, Fig. S3c). Thus, the non-apoptotic death of *Bax/Bak*$^{-/-}$ MEFs occurs in a different manner from starvation-induced cell death. Furthermore, although autophagic proteins are required, their role shows considerable differences between nutrient starvation and non-apoptotic death of *Bax/Bak*$^{-/-}$ cells.

Non-apoptotic (type II-like) death was observed in *Bax/Bak*$^{-/-}$ MEFs irrespective of their immortalization and was also seen in *Bax/Bak*$^{-/-}$ thymocytes. However, whether other normal cells also have the potential to undergo type II-like death requires further investigation. Among the cultured cell lines tested so far, overexpression of Bcl-2 did not sensitize HeLa, Jurkat or HCT116 cells to etoposide-induced non-apoptotic death (data not shown). Non-apoptotic death potential could be restricted to certain cells in the *in vitro* setting. As previously suggested[10], many cancer cells might have lost the ability to undergo non-apoptotic death as a growth advantage.

How does the Bcl-2 family of proteins regulate the non-apoptotic death? Overexpression of proteins in the BH (Bcl-2 homology) 3 subfamily (BH3-only proteins) did not induce the non-apoptotic death in *Bax/Bak*$^{-/-}$ MEFs (see Supplementary Information, Fig. S4), indicating that activation of BH3-only proteins is not sufficient to produce this form of cell death. Because Beclin 1 is required for the non-apoptotic death of *Bax/Bak*$^{-/-}$ cells and because Bcl-2/Bcl-x_L (but not Bax/Bak) binds to Beclin 1 (ref. 12), Bcl-2/Bcl-x_L might influence the creation of autophagosomes at least partly by regulation of Beclin 1. This notion is supported by the fact that the apoptotic stimulus-dependent increase of APG5–APG12 in *Bax/Bak*$^{-/-}$ MEFs (which was regulated by Beclin 1) was markedly reduced by silencing Bcl-x. This hypothesis certainly needs to be tested by using mutants of Bcl-2/Bcl-x_L and Beclin 1 that fail to interact with each other.

Anti-apoptotic Bcl-2/Bcl-x_L and pro-apoptotic Bax/Bak regulate apoptosis in opposite directions by acting on each other as well as by influencing other molecules, so the balance between these proteins is a crucial determinant of whether or not apoptosis occurs[3]. The fact that *Bax/Bak*$^{-/-}$ MEFs, in which anti-apoptotic Bcl-2 family members dominate over pro-apoptotic members, and Bcl-2/Bcl-x_L-overexpressing MEFs undergo the non-apoptotic death, suggests that the balance between Bcl-2/Bcl-x_L and Bax/Bak is also crucial for determining the occurrence of the non-apoptotic death. It has previously been described that some Bcl-2 family members can reverse their death-regulating activities, depending on expression levels or cellular contexts[13–16]. Overexpression of Bcl-2 has been reported to promote cell death from different mechanisms, for example, via proteolytic cleavage with caspases[15] or via interaction with an orphan nuclear receptor Nur77 (ref. 16). Therefore, the possibility was not formally excluded that an important role of Bcl-2/Bcl-x_L in the non-apoptotic death is dependent on this cryptic pro-death activity.

In conclusion, these findings demonstrate a previously unknown role of the Bcl-2 family in the regulation of non-apoptotic (type II-like) programmed cell death, in addition to the well-known role of this protein family in apoptosis. □

METHODS

Antibodies and chemicals. Anti-mouse Bcl-2, anti-Beclin 1 and anti-GAPDH (6G7) monoclonal antibodies were obtained from BD Biosciences (San Jose, CA). Anti-Lamin B1 and anti-VDAC monoclonal antibodies were purchased from Zymed (San Francisco, CA) and Calbiochem (La Jolla, CA), respectively. Anti-Bcl-x (L-19) polyclonal antibody was obtained from Santacruz Biotechnology (Santa Cruz, CA). Anti-APG5 polyclonal antibody was described previously[9]. 3-MA and Cell Titer Blue were obtained from ICN Biochemicals (Irvine, CA) and Promega (Madison, WI), respectively. Other chemicals were purchased from Wako (Osaka, Japan).

Cell culture and DNA transfection. Primary and SV40 T antigen-transformed WT and *Bax/Bak*$^{-/-}$ MEFs were grown in Dulbecco's modified Eagle's medium (DMEM). Apaf-1-deficient and caspase-9-deficient MEFs and their control MEFs (provided by X. Wang and K. Kuida, respectively) were also grown in the same medium. DNAs encoding human Bax, human Bak, human Bcl-2 and human Bcl-x_L in the pUC-CAGGS expression vector[17] were used. The GFP–LC3 expression construct was described elsewhere[8]. Cells (1×10^6) were transfected with plasmid DNA using the Amaxa electroporation system according to the supplier's protocol (kit V, program U-20). The transfection efficiency was more than 75% as assessed by co-transfection with DNA expressing GFP. All the siRNAs were produced by Dharmacon Research. The sequences used were as follows (numbers in parentheses indicate nucleotide positions within the respective open reading frame): mouse *Bcl-x* siRNA, 5′-AAGGAUACAGCUGGAGUCAGU-3′ (59–79); mouse *Bcl-2* siRNA, 5′-AAGUACAUACAUUAUAAGCUG-3′ (49–69); mouse *Bax* siRNA, 5′-AACAGAUCAUGAAGACAGGGG-3′ (50–70); mouse *Beclin 1* siRNA, 5′-AAGAUCCUGGACCGGGUCACC-3′ (91–111); mouse *APG5* siRNA, 5′-AACUUGCUUUACUCUCUCUAUCA-3′ (51–71). Cells (1×10^6) were transfected with 10 μg of siRNA using the Amaxa electroporation system. In the case of transfection with complementary DNA and siRNA, cDNAs (1 μg) were transfected, and after 24 h siRNAs (10 μg) were introduced.

Cell viability assay. Cells (3.5×10^6 per well) were seeded into 6-well dishes. After 24 h, the cells were treated with etoposide (20 μM) or staurosporine (1 μM) in the presence or absence of zVAD-fmk (100 μM) or 3-MA (10 mM). PI (2 μM) was added into the medium, and cells were observed under a BX50 fluorescence microscope (Olympus, Tokyo, Japan). In another experiments, all of the cells, including floating cells, were collected and viability was assessed by nuclear morphology after Hoechst 33342 (Ho342) staining, or the CTB assay. Briefly, cells were stained with 1 μM Ho342 for 5 min at room temperature, and were analysed with a fluorescence microscope (Olympus, BX50). The CTB assays were performed using CTB assay reagent, according to the supplier's protocols.

To examine the proliferation ability, MEFs were treated with etoposide or staurosporine, all the cells were recovered and 5,000 or 10,000 cells were re-cultured in standard medium into 96-well or 48-well dishes, respectively. Viable cell numbers were measured on the indicated days by the CTB assay. In the clonogenicity assay, MEFs were treated with etoposide or staurosporine, collected, and 2,000 cells were seeded in standard medium into 24-well dishes. After one week, colony numbers were counted.

Staining of autophagosomes. Cells were transfected with 1 μg of GFP–LC3 expression plasmid[8]. After 24 h, cells were treated with etoposide or staurosporine, and the fluorescence of GFP–LC3 was observed under a confocal fluorescence microscope (LSM 510 META, Zeiss, Thornwood, NY).

Electron microscopy. Cells were fixed with 2% paraformaldehyde/2% glutaraldehyde in 0.1 M phosphate buffer (pH 7.4), followed by 1% OsO_4. After dehydration, thin sections were stained with uranyl acetate and lead citrate for observation under a JEM 100 CX electron microscope (JEOL, Peabody, MA).

Note: Supplementary Information, Information is available on the Nature Cell Biology website.

ACKNOWLEDGEMENTS

We are grateful to S. J. Korsmeyer for providing SV40-immortalized *Bax/Bak*$^{-/-}$ MEFs. This study was supported in part by grants for Scientific Research on Priority Areas, Center of Excellence Research, the twenty-first century COE Program, and Scientific Research, from the Ministry of Education, Science, Sports and Culture of Japan, and by a grant for Research on Dementia and Fracture from the Ministry of Health, Labour and Welfare of Japan.

COMPETING FINANCIAL INTERESTS

The authors declare that they have no competing financial interests.

Received 12 July 2004; accepted 5 October 2004
Published online at http://www.nature.com/naturecellbiology.

1. Baehrecke, E. H. How death shapes life during development. *Nature Rev. Mol. Cell Biol.* **3,** 779–787 (2002).
2. Clarke, P. G. Developmental cell death: morphological diversity and multiple mechanisms. *Anat. Embryol. (Berl.)* **181,** 195–213 (1990).
3. Tsujimoto, Y. Cell death regulation by the Bcl-2 protein family in the mitochondria. *J. Cell. Physiol.* **195,** 158–167 (2003).
4. Lindsten, T. *et al.* The combined functions of proapoptotic Bcl-2 family members bak and bax are essential for normal development of multiple tissues. *Mol. Cell* **6,** 1389–1399 (2000).
5. Wei, M. C. *et al.* Proapoptotic BAX and BAK: a requisite gateway to mitochondrial dysfunction and death. *Science* **292,** 727–730 (2001).
6. Zong, W. X., Lindsten, T., Ross, A. J., MacGregor, G. R. & Thompson, C. B. BH3-only proteins that bind pro-survival Bcl-2 family members fail to induce apoptosis in the absence of Bax and Bak. *Genes Dev.* **15,** 1481–1486 (2001).
7. Bursch, W. The autophagosomal-lysosomal compartment in programmed cell death. *Cell Death Differ.* **8,** 569–581 (2001).
8. Kabeya, Y. *et al.* LC3, a mammalian homologue of yeast Apg8p, is localized in autophagosome membranes after processing. *EMBO J.* **19,** 5720–5728 (2000).
9. Mizushima, N. *et al.* Dissection of autophagosome formation using Apg5-deficient mouse embryonic stem cells. *J. Cell Biol.* **152,** 657–668 (2001).
10. Liang, X. H. *et al.* Induction of autophagy and inhibition of tumorigenesis by beclin 1. *Nature* **402,** 672–676 (1999).
11. Kihara, A., Kabeya, Y., Ohsumi, Y. & Yoshimori, T. Beclin-phosphatidylinositol 3-kinase complex functions at the trans-Golgi network. *EMBO Rep.* **2,** 330–335 (2001).
12. Liang, X. H. *et al.* Protection against fatal Sindbis virus encephalitis by beclin, a novel Bcl-2-interacting protein. *J. Virol.* **72,** 8586–8596 (1998).
13. Chen, J. *et al.* bcl-2 overexpression reduces apoptotic photoreceptor cell death in three different retinal degenerations. *Proc. Natl Acad. Sci. USA* **93,** 7042–7047 (1996).
14. Fannjiang, Y. *et al.* BAK alters neuronal excitability and can switch from anti- to pro-death function during postnatal development. *Dev. Cell* **4,** 575–585 (2003).
15. Cheng, E. H. *et al.* Conversion of Bcl-2 to a Bax-like death effector by caspases. *Science* **278,** 1966–1968 (1997).
16. Lin, B. *et al.* Conversion of Bcl-2 from protector to killer by interaction with nuclear orphan receptor Nur77/TR3. *Cell* **116,** 527–540 (2004).
17. Shimizu, S., Eguchi, Y., Kamiike, W., Matsuda, H. & Tsujimoto, Y. Bcl-2 expression prevents activation of the ICE protease cascade. *Oncogene* **12,** 2251–2257 (1996).
18. Kuma, A. *et al.* The role of autophagy during the early neonatal starvation period. *Nature* (in the press).

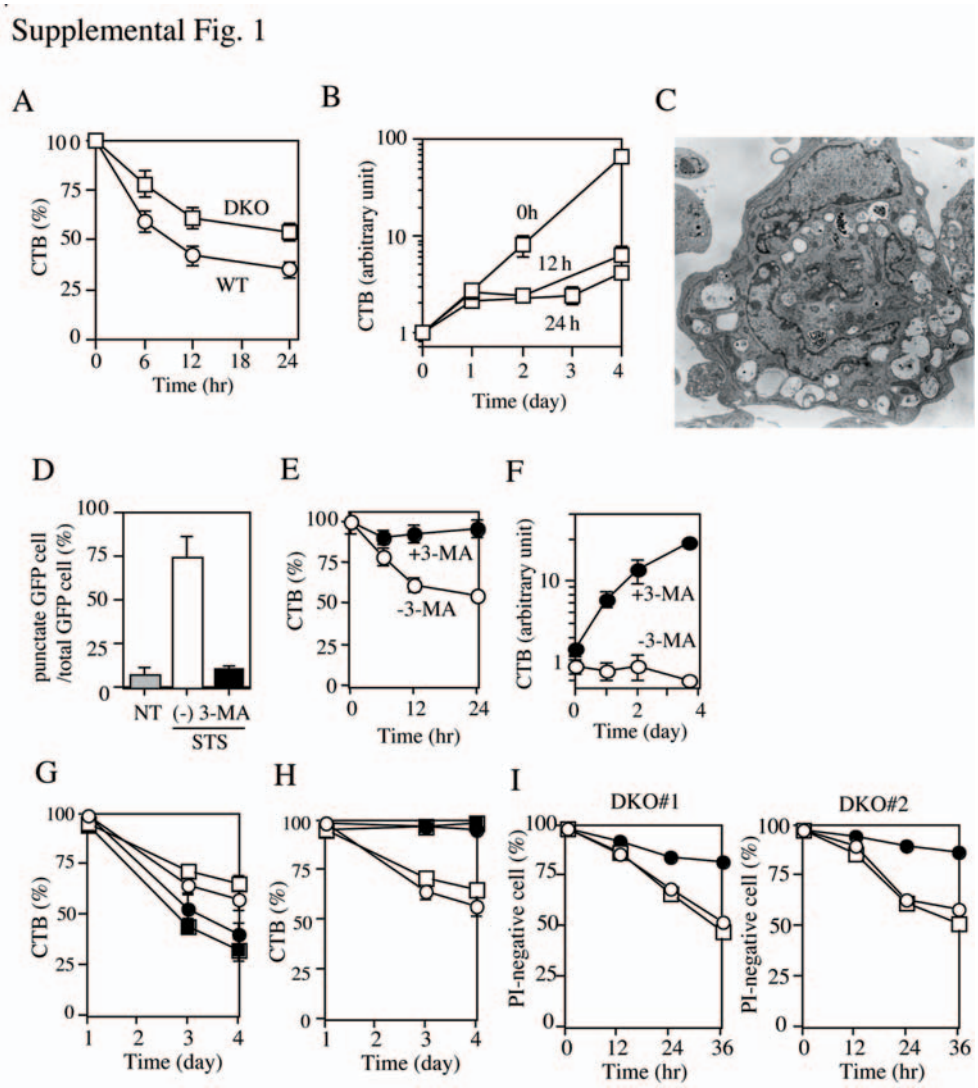

Figure S1 Induction of non-apoptotic death of SV40-transformed and primary DKO MEFs, and DKO thymocytes. (A-F) STS-induced non-apoptotic death of DKO MEF. (A, B) Reduced viability of DKO MEFs after exposure to STS. WT and DKO MEFs were treated with 1 μM STS. Then cell viability was measured (A) by the CTB assay and (B) by the same procedure as in (Fig. 1D). Data are shown as mean ± SD (n=4). (C) Electron micrograph of DKO MEFs treated with STS (x 17,000). Cells were incubated with STS (1 μM) for 12 hours, and then examined by electron microscopy. (D-F) Inhibition of STS-induced death of DKO MEFs by blocking autophagy. (D) GFP-LC3-transfected DKO MEFs were treated with 1 μM STS in the absence or presence of 10 mM 3-MA. The percentage of cells with punctate GFP-LC3 fluorescence was calculated relative to all GFP-LC3-positive cells. (E, F) DKO MEFs were treated with 1 μM STS in the absence or presence of 10 mM 3-MA for the indicated times (E) and 12 hr (F). Cell viability was measured by the CTB assay (E), and cell proliferation assay (F). Data are shown as mean ± SD (n=4). (G-I) Induction of non-apoptotic death of primary DKO MEFs and DKO thymocytes. (G) Reduced viability of primary DKO MEFs after exposure to etoposide. WT (closed squares), Bak-/- (closed circles) and DKO#1, 2 (open circles and squares, respectively) primary MEFs were treated with 50 μM etoposide. Then cell viability was measured by the CTB assay, and expressed as a percentage of the value at 1 day after etoposide treatment. This was because all the primary MEFs proliferated normally for 1 day after etoposide treatment (approximately 4-fold increase in cell numbers). (H) Inhibition of etoposide-induced cell death by 3-MA. Primary DKO MEFs (#1, #2) were treated with 50 μM etoposide in the absence (open symbols) or presence of 10 mM 3-MA (closed symbols) for the indicated day. Cell viability was measured by the CTB assay. (I) Reduced viability of DKO thymocytes after exposure to STS. DKO thymocytes (isolated from 2 different mice #1 and #2) were treated with 0.5 μM STS in the absence (open squares) or presence of 100 μM zVAD-fmk (open circles), or 10 mM 3-MA (closed circles). Then cell viability was measured by the PI staining and expressed as the percentage of PI-negative cells per total cells.

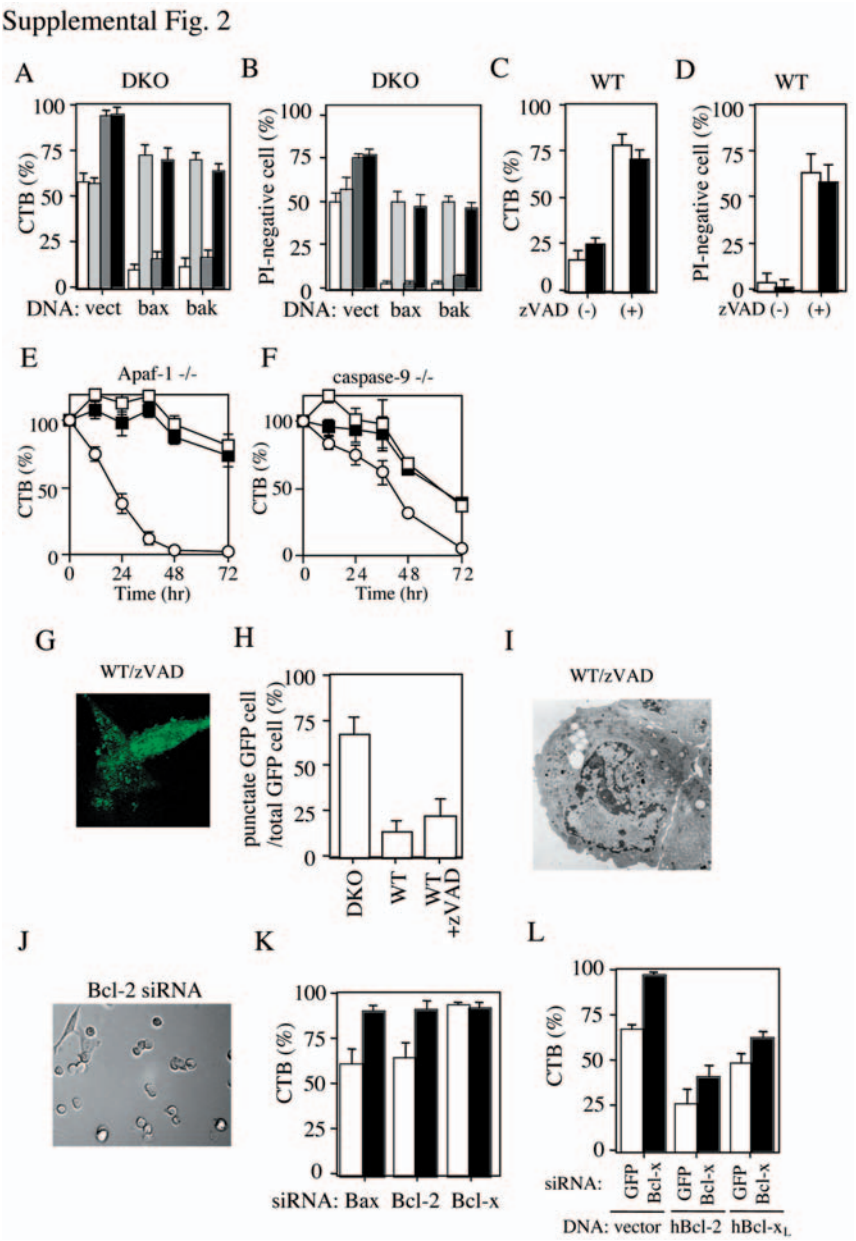

Figure S2 Absence of etoposide-induced 3-MA-inhibitable non-apoptotic death in MEFs by caspase inhibition, and no inhibition of non-apoptotic death in etoposide-treated DKO MEFs by siRNA for Bcl-2. (A-I) Absence of etoposide-induced 3-MA-inhibitable non-apoptotic death in MEFs by caspase inhibition. (A, B) DKO MEFs were transiently transfected with 1 μg of the indicated DNAs. After 24 hours, cells were treated with 20 μM etoposide in the absence (white columns) or presence of 100 μM zVAD (gray columns), 10 mM 3-MA (darkgray columns), or 100 μM zVAD plus 10 mM 3-MA (black columns), and then cell viability was measured by the CTB assay after 24 hours (A) and PI staining after 48 hours (B). Data are shown as mean ± SD for n=4. (C, D) Failure of 3-MA to inhibit death of WT MEFs treated with etoposide in the presence of a caspase inhibitor. WT MEFs with (closed columns) or without (open columns) 10 mM 3-MA were treated with etoposide in the absence or presence of 100 μM zVAD-fmk, and then cell viability was measured by the CTB assay after 24 hours (C) and PI staining after 48 hours (D). Data are shown as mean ± SD (n=4). (E, F) No effect of 3-MA on cell viability in Apaf-1- and caspase-9-deficient MEFs treated with etoposide. Apaf-1-deficient and caspase-9-deficient (squares) and their control MEFs (circles) were treated with 20 μM etoposide in the absence (open symbols) or presence (closed symbols) of 10 mM 3-MA, and then cell viability was assessed by the CTB assay. Data are shown as mean ± SD (n=4). (G-I) Mild induction of autophagy in MEFs after etoposide treatment. (G, H) WT MEFs that were transfected with GFP-LC3 were incubated with 20 μM etoposide in the absence or presence of 100 μM zVAD for 24 hours, and then were examined by confocal fluorescent microscopy. A representative photograph is shown (G), in which cells exhibit mild punctate distribution of GFP-LC3. The percentage of cells with punctate GFP-LC3 fluorescence was calculated relative to all GF-LC3-positive cells (H). Data are shown as mean ± SD. (I) WT MEFs were incubated with 20 μM etoposide in the presence of 100 μM zVAD for 18 hours, and then were analysed by electron microscopy (x 8,500). (J-L) No inhibition of non-apoptotic death in etoposide-treated DKO MEFs by siRNA for Bcl-2. (J) DKO MEFs that were transfected with the siRNA for Bcl-2 were treated with 20 μM etoposide for 24 hours, and then were examined by phase-contrast microscopy. (K) DKO MEFs that were transfected with the indicated siRNAs were treated with 20 μM etoposide in the absence (open symbols) or presence (closed symbols) of 10 mM 3-MA, and cell viability was assessed by the CTB assay at 24 hours. Data are presented as mean ± SD (n=4). (L) DKO cells that were transfected with the indicated siRNA together with plasmid (vector, human Bcl-2 or human Bcl-x_L) were treated with 20 μM etoposide for 24 hr and then cell viability was assessed by the CTB assay. Data are presented as mean ±SD (n=3).

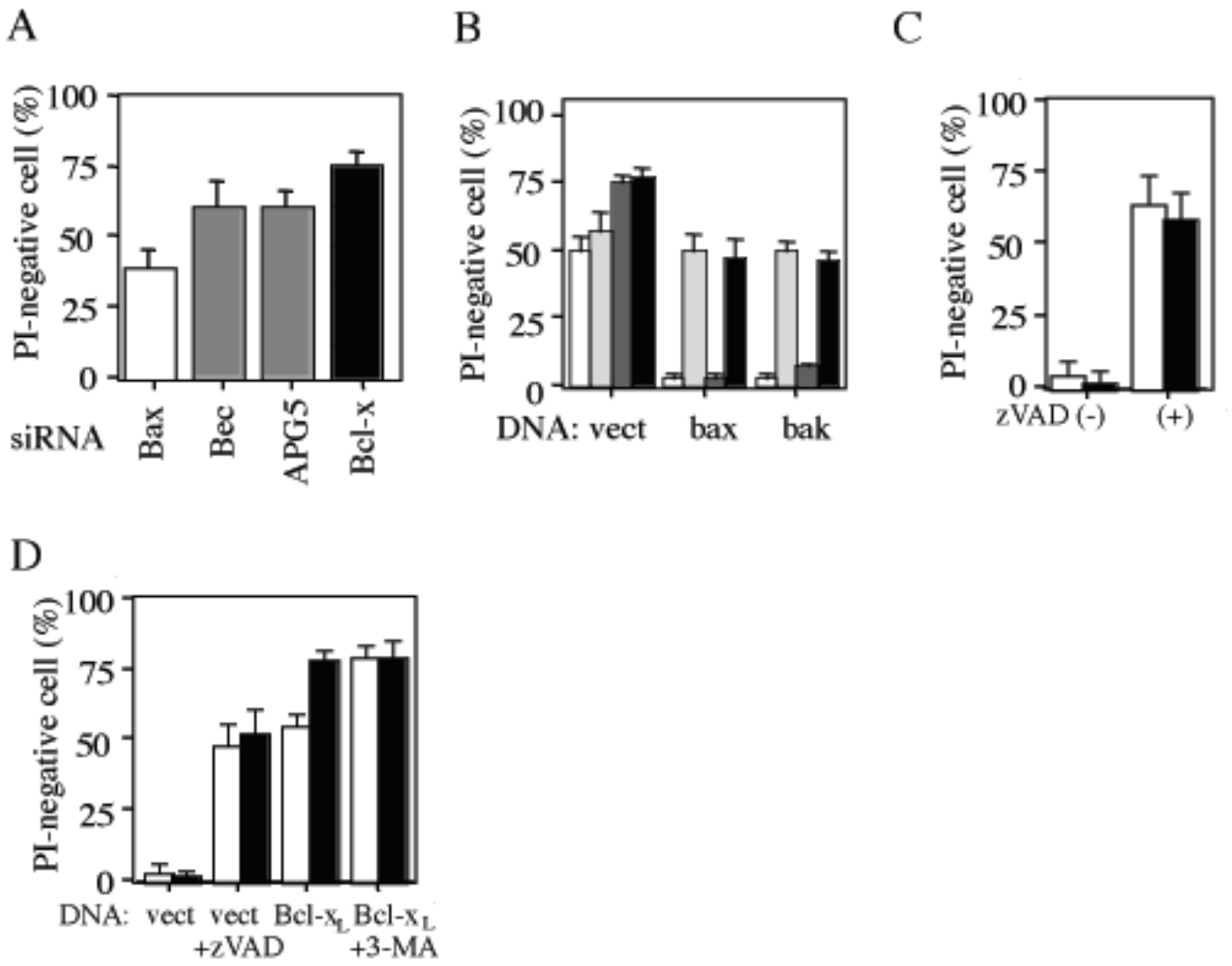

Figure S3 Assessment of cell viability by the PI staining **(A)** Inhibition of etoposide-induced death of DKO MEFs by silencing of Beclin 1, APG5, and Bcl-x. DKO MEFs which were treated with the indicated siRNAs were incubated with 20 μM etoposide for 48 hours. Cell viability was measured by PI staining. Data are shown as mean ± SD (n=3). **(B)** Similar experiments as shown in Fig. 3A were performed, and cell viability was assessed by PI staining after 48 hours. White columns: no inhibitor, gray columns: 100 μM zVAD, darkgray columns: 10 mM 3-MA, or black columns:100 μM zVAD plus 10 mM 3-MA. Data are shown as mean ± SD for n=3. **(C)** Similar experiments as shown in Fig. 3B were performed, and cell viability was assessed by PI staining after 48 hours. White columns: 3-MA (-), black columns: 10 mM 3-MA. **(D)** Similar experiments as shown in Fig. 3J were performed, and cell viability was assessed by PI staining after 48 hours. White columns: APG+/+ MEFs, black columns: APG-/- MEFs.

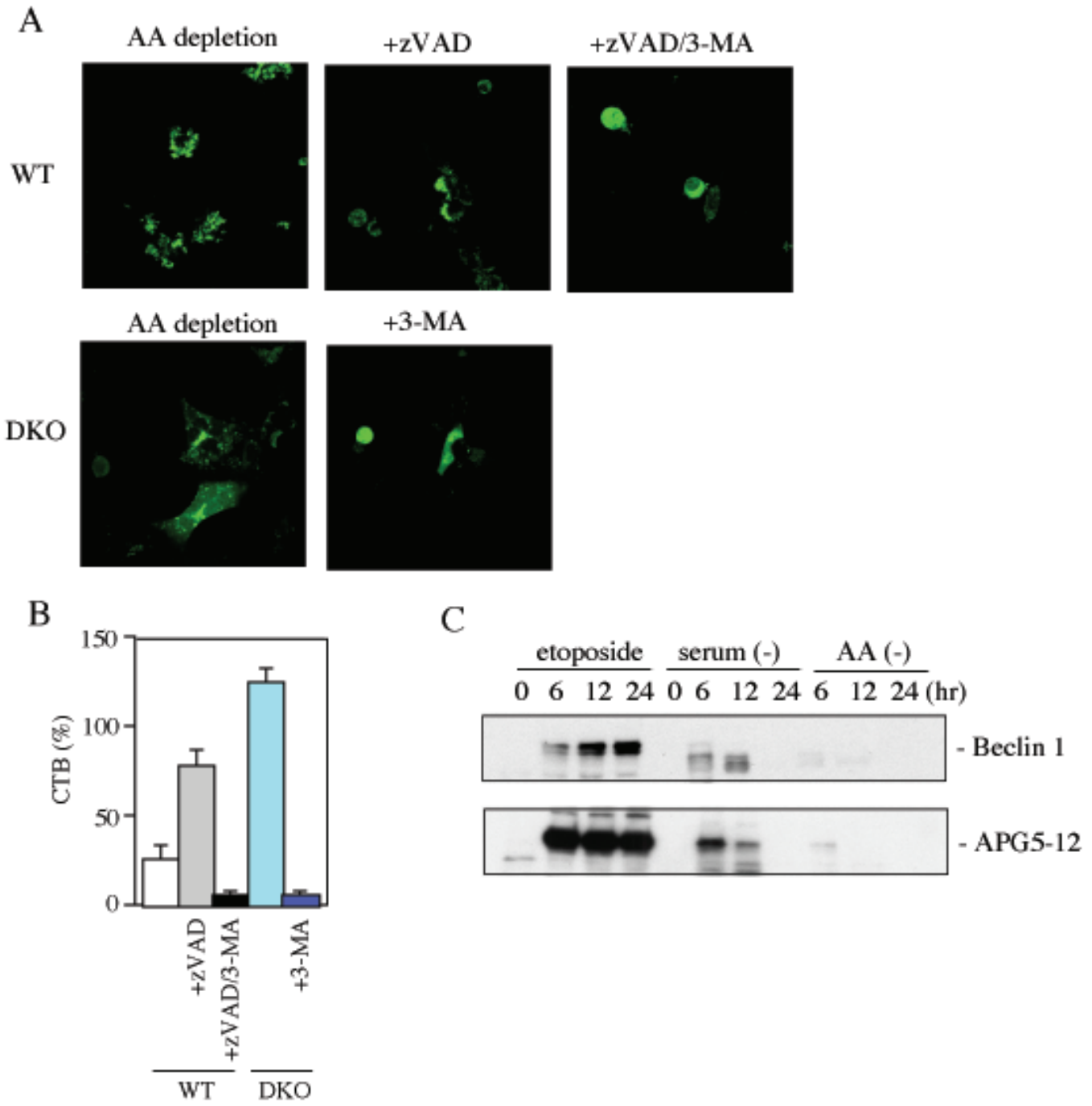

Figure S4 Apoptotic death of MEFs by amino acid starvation. **(A)** 3-MA-inhibitable punctate GFP-LC3 fluorescence in WT and DKO MEFs after deprivation of amino acids. WT and DKO MEFs that were transfected with GFP-LC3 were cultured in the starvation medium (Hanks balanced solution supplemented with 10% glucose, 1 mM sodium pyruvate, 10 mM Hepes/Na^+, (pH 7.4), 0.05 mM 2-mercaptoethanol, 100 U/ml penicillin, and 100 µg/ml streptomycin) with or without 10 mM 3-MA and/or 100 µM zVAD-fmk for 24 hours, and then were examined by confocal fluorescent microscopy. Representative photographs are shown. Both WT and DKO MEFs showed punctate GFP-LC3 fluorescence, which were inhibited by 3-MA, **(B)** Death of WT and DKO MEFs by amino acid starvation. WT and DKO MEFs were cultured in the starvation medium with or without 10 mM 3-MA and/or 100 µM zVAD-fmk. After 24 hours, cells were harvested and cell viability was assessed by CTB assay. Similar results were also obtained with PI staining. **(C)** No accumulation of Beclin 1 and APG5-APG12 complex in DKO MEFs after starvation. DKO MEFs were incubated with normal medium with 20 µM etoposide, serum-depleted medium (which also activates autophagy), and starvation medium for 24 hours. Expression of Beclin 1 and APG5-APG12 complex was analysed by Western blot analysis.

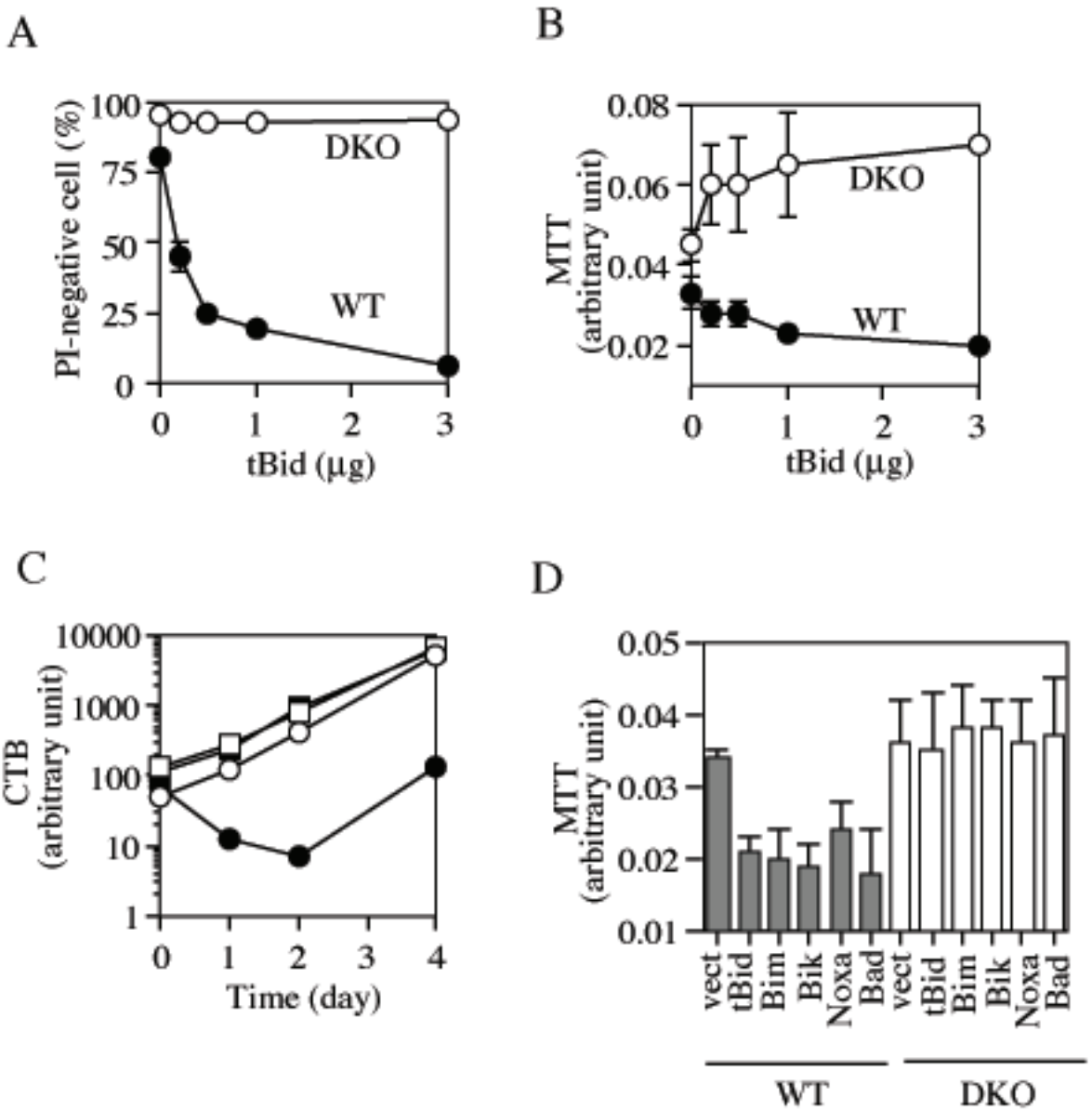

Figure S5 DKO MEFs died by etoposide, but not by BH3-only proteins. **(A, B)** WT (closed circles) and DKO MEFs (open circles) were transfected with the indicated amounts of tBid expression DNA, and cell viability was assessed by PI staining (A) and the MTT assay (B) at 24 hours. The CTB assay gave the virtually identical results as those with the MTT assay. **(C)** WT (closed symbols) and DKO (open symbols) MEFs were transfected with 3 µg of tBid expression DNA (circles) or control vector (squares), and viable cell numbers were measured by the CTB assay at the indicated times. Data are shown as mean ± SD (n=4). **(D)** No death of DKO MEFs by various BH3-only proteins. WT and DKO MEFs were transfected with 1 µg of the expression DNA for the indicated proteins, and cell viability was assessed by the MTT assay at 24 hours. Data are shown as mean ± SD (n=4).

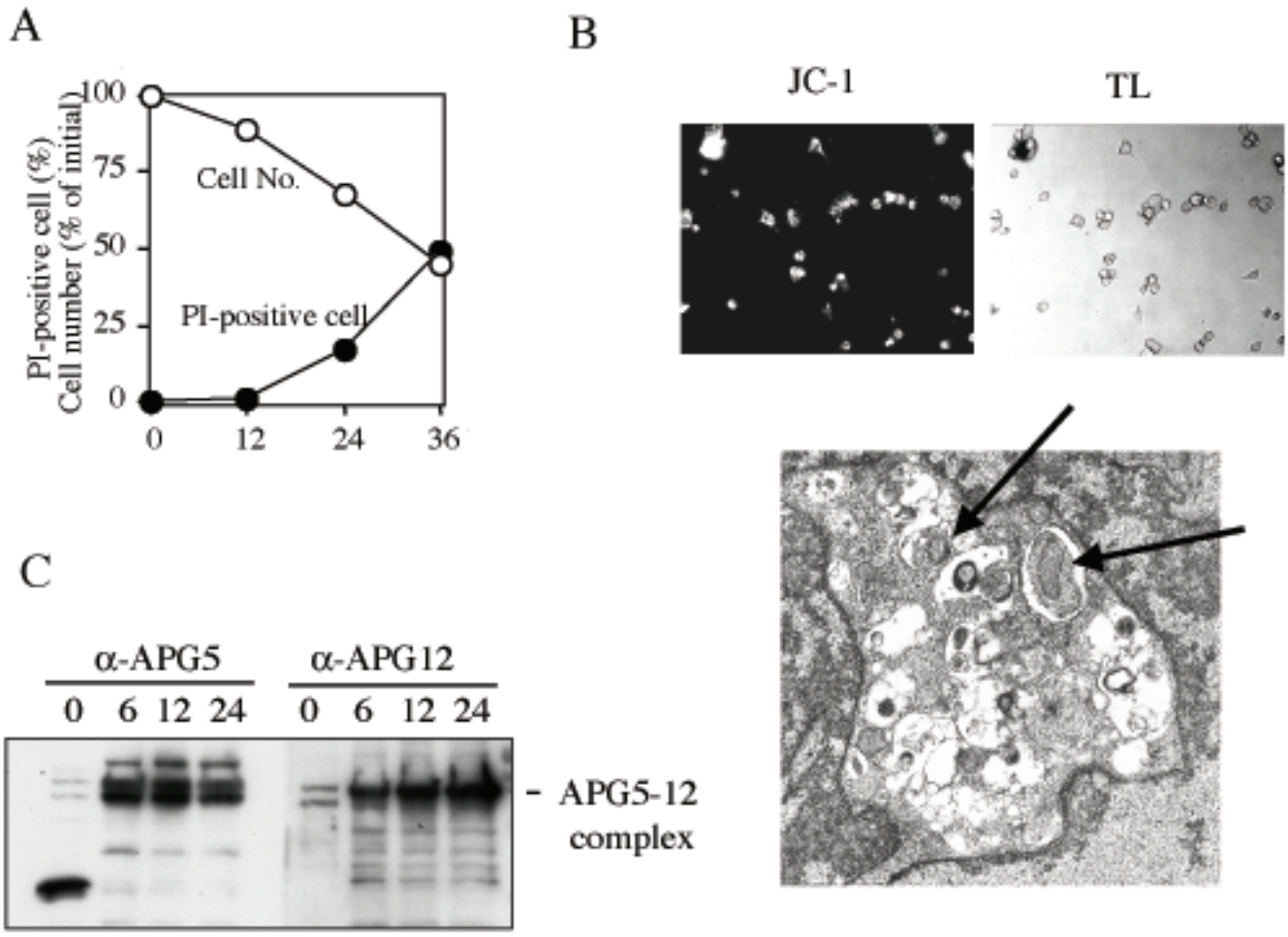

Figure A. Loss of etoposide-treated DKO MEFs in flow cytometric analysis. DKO MEFs were treated with 20 μM etoposide, and PI-positive cells were counted under fluorescence microscope. Cells were also harvested and the number of cell was counted by flow cytometer. **Figure B. Maintenance of mitochondrial membrane potential in etoposide-treated DKO MEFs.** (upper panel) DKO MEFs were treated with 20 μM etoposide for 36 hours, stained with JC-1 (10 μM), and the red fluorescence was observed under a fluorescence microscope. (Lower panel) DKO MEFs were treated with 20 μM etoposide for 18 hours, and analysed by electron microscopy. As shown in an EM photograph, some mitochondria were found in autophagosomes (arrows). **Figure C. Production of APG5/12 complex in etoposide-treated DKO MEFs** DKO MEFs were treated with 20 μM etoposide for the indicated hours. Expression of APG5/12 complex was analyzed by Western blot analysis using anti-APG5 and APG12 antibodies. Both antibodies reacted with the same band.

Movie 1 Phase-contrast microscopic analysis of etoposide-treated DKO MEFs. DKO MEFs were treated with 20 μM etoposide and observed for 40 hours under a phase-contrast microscope. Cells rounded around 12-18 hr, ruffled around 18-30 hr, and ballooned around 24-40 hr.
Movies 2, 3 Phase-contrast and PI-staining analysis of etoposide-treated DKO MEFs. DKO MEFs were treated with 20 μM etoposide in the presence of 2 μM PI and observed from 8 hours to 36 hours under a phase-contrast (2) and fluorescence (3) microscope.

Movies 4, 5 Phase-contrast microscopic and PI-staining analysis of etoposide-treated DKO MEFs with 3-MA. DKO MEFs were treated with 20 μM etoposide plus 10 μM 3-MA in the presence of 2 μM PI and observed from 12 hours to 48 hours under a phase-contrast (6) and fluorescence (7) microscope. The number of PI-positive cells was greatly reduced compared with that in Movie 3